over another in performing a specific kind of computation (*22*).

In conclusion, the enhanced performance of IC-related tasks below the horizontal meridian indicates that physiological studies and theoretical models of scene segmentation should take into account early cortical processing inhomogeneities and functional specialization. In addition, testing other visual tasks (for example, perceptual grouping) for up/down asymmetry may help to establish relations between the different components of visual processing.

REFERENCES AND NOTES

1. G. Kanizsa, *Organization in Vision* (Praeger, New York, 1979); E. Peterhans and R. von der Heydt, *Trends. Neurosci.* **14**, 112 (1991); S. Petry and G. E. Meyer, Eds., *The Perception of Illusory Contours* (Springer, New York, 1987).
2. L. H. Finkel and P. Sajda, *Neural Networks* **6**, 901 (1992); S. Grossberg and E. Mingolla, *Psychol. Rev.* **92**, 173 (1985); F. Heitger and R. von der Heydt, *Proc. Int. Conf. Comp. Vision* **4**, 32 (1993); M. Nitzberg, D. Mumford, T. Shiota, *Filtering, Segmentation and Depth* (Springer, New York, 1993); S. Ullman, *Biol. Cybern.* **25**, 1 (1976); L. R. Williams and D. W. Jacobs, *Proc. Int. Conf. Comp. Vis.* **5**, 408 (1995).
3. R. von der Heydt, E. Peterhans, G. Baumgartner, *Science* **224**, 1260 (1984); R. von der Heydt and E. Peterhans, *J. Neurosci.* **9**, 1731 (1989); E. Peterhans and R. von der Heydt, *ibid.*, p. 1749.
4. In extrastriate cortical areas (V2 and higher) of humans and other primates, the upper and lower visual quadrants are represented, respectively, on the lower and upper parts of the cortical sheet within each hemisphere, with visual area V1 physically separating them [D. J. Felleman and D. C. van Essen, *Cereb. Cortex* **1**, 1 (1991); J. C. Horton and W. F. Hoyt, *Arch. Ophthalmol.* **109**, 816 (1991)]. In human neurological patients, this can lead to pronounced quadrantic field defects—a sharp change in visual capacity across the horizontal meridian [G. Holmes, *Proc. R. Soc. London Ser. B.* **132**, 348 (1945); J. C. Horton and W. F. Hoyt, *Brain* **114**, 1703 (1991)].
5. The stereoscopic stimulus was presented with the use of a prism stereo viewer (11 subjects) or as a red/green anaglyph (15 subjects) [B. Julesz, *Foundations of Cyclopean Vision* (Univ. of Chicago Press, Chicago, 1971)].
6. The four remaining subjects could not discern a perceptual difference between the two fixation conditions.
7. In that respect, the stimulus of Fig. 2 is different from most other stereograms involving an illusory occluder [for example, S. Blomfield, *Nature New Biol.* **245**, 256 (1973)], because an (illusory) edge in any orientation other than the horizontal would result in a disparity in the left- and right-eye images for which the only ecologically valid interpretation is one of there being an illusory occluder.
8. D. Ringach and R. Shapley, *Perception (suppl.)* **22**, 51 (1993).
9. Subjects CT and CH were naïve about the purpose of the experiment. All subjects received extensive practice in performing the shape-discrimination task with the stimulus centered around the fixation point before the collection of the data presented.
10. The stimulus subtended a visual angle of 2.75° and was centered 3.4° above or below the fixation point. The stimulus was presented for 83 ms, followed by a blank screen for 83 ms and then by a mask for 250 ms. The stimulus and the mask were white (12 cd/m^2) on a dark background. The subject was restrained with a chin and forehead rest, and the experiment room was dark.
11. A sigmoid curve ($\{1 + \tanh[b(x - a)]\}/2$) was fit to the data of each psychometric function, with the slope (b) and bias (a) as free parameters; the thresholds were computed from the fitted curves.
12. The differences in thresholds between the upper and lower visual hemifields were statistically significant in the IC condition (Fig. 3A) for all subjects. The differences in the two control conditions were not significant for any of the subjects. The error bars of the slopes (b) were estimated from the variance-covariance matrix [R. Fletcher, *Practical Methods of Optimization* (Wiley, New York, 1980)].
13. For the two presentation conditions (upper and lower hemifields), the stimuli were mirror-reflected about a horizontal line passing through the center, such that in both cases the inducers' arcs were facing the fixation point.
14. N. Rubin, K. Nakayama, R. Shapley, data not shown.
15. B. Breitmeyer, B. Julesz, W. Kropfl, *Science* **187**, 269 (1975); B. Julesz, B. Breitmeyer, W. Kropfl, *Perception* **5**, 129 (1976). Breitmeyer *et al.* found an up/down anisotropy and right-left isotropy in the detection of dynamic stereoscopic targets. Their results, however, may be accounted for by the fact that the vertical horopter does not lie on the frontoparallel plane [C. Tyler, in *Binocular Vision*, D. Regan, Ed. (CRC Press, Boca Raton, FL, 1991)].
16. J. C. Anderson, K. A. C. Martin, D. Whitteridge, *Cereb. Cortex* **3**, 412 (1993); C. D. Gilbert, *ibid.*, p. 373; J. S. Lund, T. Yoshioka, J. B. Levitt, *ibid.*, p. 148.
17. This raises the possibility that the differential specialization in scene segmentation reported here may in turn be related to functional specialization of higher visual areas in the ventral and dorsal streams [L. G. Ungerleider and M. Mishkin, in *Analysis of Visual Behavior*, D. J. Ingle, M. A. Goodale, R. J. W. Mansfield, Eds. (MIT Press, Cambridge, MA, 1982); M. A. Goodale and A. D. Milner, *Trends Neurosci.* **15**, 20 (1992)], because the lower and upper parts of early visual areas project more to ventral and dorsal areas outside the occipital lobe, respectively [J. H. R. Maunsell and W. T. Newsome, *Annu. Rev. Neurosci* **10**, 363 (1987); (*19*)].
18. J. J. Gibson, *The Perception of the Visual World* (Houghton Mifflin, Boston, 1950); K. Nakayama and S. Shimojo, *Science* **257**, 1357 (1992).
19. F. Previc, *Behav. Brain Sci.* **13**, 519 (1990).
20. M. D. Lezak, *Neuropsychological Assessment* (Oxford Univ. Press, New York, 1995), pp. 405–407; J. Wasserstein, R. Zappula, J. Rosen, L. Gerstman, *Brain Cognition* **3**, 51 (1984); ———, D. Rock, *ibid.* **6**, 1 (1987).
21. J. Hirsch *et al.*, *Proc. National Acad. Sci. U.S.A.* **92**, 6469 (1995); B. Gulyas and P. Roland, in *Functional Organization of Human Visual Cortex*, B. Gulyas, D. Ottoson, P. Roland, Eds. (Pergamon, New York, 1993), pp. 346–347.
22. A. Chernjavsky and J. Moody, *Neural Computation* **2**, 334 (1990); G. M. Edelman, *Neural Darwinism* (Basic Books, New York, 1987), chap. 6.

23. We thank P. Cavanagh, R. Frost, J. Hirsch, K. Miller, S. Suzuki, and S. Ullman for helpful discussions and for reviewing the manuscript. Supported by the McDonnell-Pew Program in Cognitive Neuroscience (N.R.), Air Force Office of Scientific Research grant F4 96209510036 (K.N.), and National Institutes of Health grant EY-01472 (R.S.).

28 August 1995; accepted 28 November 1995

Use-Dependent Blockers and Exit Rate of the Last Ion from the Multi-Ion Pore of a K^+ Channel

Thomas Baukrowitz and Gary Yellen*

Quaternary ammonium blockers inhibit many voltage-activated potassium (K^+) channels from the intracellular side. When applied to *Drosophila* Shaker potassium channels expressed in mammalian cells, these rapidly reversible blockers produced use-dependent inhibition through an unusual mechanism—they promoted an intrinsic conformational change known as C-type inactivation, from which recovery is slow. The blockers did so by cutting off potassium ion flow to a site in the pore, which then emptied at a rate of 10^5 ions per second. This slow rate probably reflected the departure of the last ion from the multi-ion pore: Permeation of ions (at 10^7 per second) occurs rapidly because of ion-ion repulsion, but the last ion to leave would experience no such repulsion.

Use dependence is a valuable property for therapeutic inhibitors of ion channels. The ability to block channels during periods of particularly high activity while leaving resting channels relatively unaffected makes use-dependent channel inhibitors valuable as anticonvulsant or antiarrhythmic agents (*1*). The accepted mechanism of use-dependent inhibition is that an inhibitor binds better when the channel is used and then dissociates slowly (*2*). In studying open-channel blockers of voltage-activated K^+ channels, we found a different mechanism of use dependence. Although the blockers dissociated quickly from the channel, their effect was long lasting because they promoted the intrinsic inactivation gating of the channel, which itself was slow to recover. This influence on inactivation occurred through alteration of the K^+ movements in the channel that affect inactivation rather than through an allosteric change in blocker binding to the channel. Analysis of this previously unknown mechanism of use dependence provided information about the kinetics of ion movements in the K^+ channel pore.

We used the cloned Shaker-H4 K^+ channel from *Drosophila* with a deletion mutation ($\Delta 6$–*46*) that removes the rapid N-type inactivation (*3*, *4*). These channels (ShΔ channels), expressed in mammalian cells by transient transfection, have the gating behavior of delayed rectifier K^+ channels: They activate rapidly in response to a depolarizing voltage step and then inactivate rather slowly. This inactivation occurs

Department of Neurobiology, Harvard Medical School and Massachusetts General Hospital, 50 Blossom Street, Boston, MA 02114, USA.

*To whom correspondence should be addressed.

by a distinct molecular mechanism (C-type) that produces a conformational change at the outer mouth of the pore (*4*, *5*).

We studied the action of classical quaternary ammonium blockers, which block the intracellular mouth of the channel when the activation gates are open. We began with decyltriethylammonium (C_{10}-TEA), a high-affinity blocker (*6*–*8*). After channel opening, C_{10}-TEA binds within milliseconds to the channel and blocks it; on repolarization, the drug dissociates within tens of milliseconds (*8*).

In spite of the rapid binding and dissociation of this compound, it produced (in addition to the transient blockade during each pulse) a use-dependent accumulative blockade at moderate stimulation frequency (Fig. 1, A and B). As for classical use-dependent blockade, this progressive reduction of the peak current depended on the stimulus frequency: Higher frequencies produced more reduction of the current. This was not, however, due to a classical mechanism in which recovery from blockade is slow or in which the blocker slows recovery from inactivation. Rather, the blocker speeded up entry into the normal C-type inactivated state. In the absence of the blocker, C-type inactivation occurred slowly and recovered with a time constant of 6 to 7 s (Fig. 1C). When the blocker was present, there was a very rapid decline in current caused by the onset of blockade, which was followed by an inactivation phase that was faster and more complete than normal, but recovery occurred at the normal rate (Fig. 1C). A similar effect on the onset of inactivation was observed for the mammalian Kv1.4 channel (Fig. 1D).

The overall rate of the inactivation phase that followed blockade was a weighted average between a rapid rate for the blocked channels and the normal slow rate for the unblocked channels (Fig. 1E). To determine the rate of inactivation of blocked channels, we used a high degree of blockade (>90%) and looked at the disappearance of the remaining current. The rate of inactivation of the blocked channels was very sensitive to external potassium concentration ($[K^+]$) in the physiologic range: It was fast in zero external $[K^+]$ and became much slower as $[K^+]$ increased, with an apparent affinity (K_{app}) of 2 mM (Fig. 2A). The same $[K^+]$ dependence for the rate of C-type inactivation occurs in two other situations in which the outward flow of K^+ ions is eliminated: either when the inner mouth of the pore is blocked by N-type inactivation or when all internal K^+ is temporarily removed and inactivation is monitored by measuring inward current (*9*, *10*). Our working hypothesis is that the rate of C-type inactivation is governed by the occupancy of an ion-binding site near the external mouth of the pore, and that blocking K^+ efflux starves this control site and speeds up the rate of C-type inactivation (*9*), particularly in the absence of external K^+.

This hypothesis seems to suggest that all blockers producing a given level of fractional block should have an equal effect on the

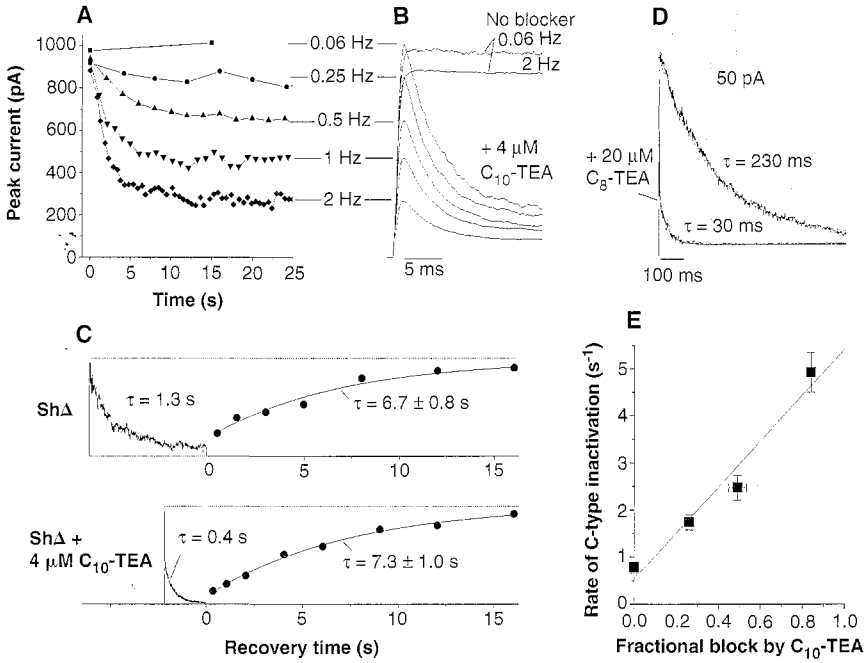

Fig. 1. Internal K^+ channel blockers produce use-dependent inhibition by speeding up C-type inactivation. (**A**) Development of use-dependent inhibition of K^- current through ShΔ channels by C_{10}-TEA. Transient currents [shown in (B)] were measured for 20-ms depolarization from −80 to 0 mV with 4 μM C_{10}-TEA on the intracellular side of the membrane. Internal $[K^-]$ = 160 mM, external $[K^-]$ = 3 mM; standard conditions (*18*). After a long resting period (about 30 s), pulses began at the indicated frequency. The initial peak current was plotted against the time elapsed since the beginning of the pulse train. (**B**) Averaged steady-state currents at the indicated stimulation frequencies. For reference, currents in the absence of blocker are shown for the highest and lowest frequencies. (**C**) C-type inactivation and recovery for control ShΔ currents (top panel) and in the presence of 4 μM C_{10}-TEA (bottom panel). The long pulse current shows the onset of inactivation; the symbols indicate the initial currents for the second pulse in a series of two-pulse recovery experiments, plotted against the time allowed for recovery between the two pulses. Best fit single exponentials are shown with the estimated time constants. The long-pulse current with blocker consists of a rapid block phase (complete within 50 ms) followed by a single-exponential inactivation phase. (**D**) Currents from rat Kv1.4 channels expressed in HEK 293 cells after oxidation to eliminate N-type inactivation (*19*). When blocker is present, the rapid C-type inactivation becomes faster. The external solution contains 150 mM NaCl and 10 mM KCl. (**E**) Dependence of C-type inactivation rate on the fractional block by C_{10}-TEA. ShΔ currents were measured [as shown in (C), bottom panel] with different blocker concentrations. The inactivation rate (second relaxation phase) is plotted as a function of the fractional steady-state block within a single pulse. The linear dependence is consistent with the overall rate being the weighted average of a slow rate for the unblocked channels and a fast rate for the blocked channels.

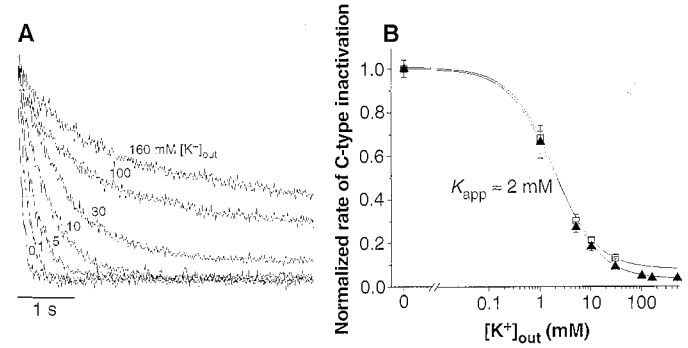

Fig. 2. Blocker effects on C-type inactivation involve a K^+ site. (**A**) C-type inactivation in the presence of 10 μM C_{10}-TEA with various external $[K^+]$ ($[K^+]_{out}$). All currents have a rapid initial block phase during which the currents are blocked by 90%. The remaining current is expanded and normalized to show the C-type inactivation phase. (**B**) $[K^+]$ dependence of C-type inactivation rate in the presence of blocker for C_{10}-TEA (solid triangles) and C_4-TEA (open squares). Rates are normalized to the maximum rate with zero external $[K^-]$ and fitted to the equation $R = [1 + R_{min}([K^-]/K_{app})]/[1 + ([K^+]/K_{app})]$; the two best fit values for K_{app} were both about 2 mM.

inactivation rate. However, even for a series of closely related alkyltriethylammonium blockers, there was substantial variation in the effect on the C-type inactivation rate (Fig. 3, A and B). We observed the maximal effect of the blockers with zero external $[K^+]$ and normal internal $[K^+]$. The compounds showed various degrees of enhancement (from 2- to 10-fold), except for TEA, which had little or no effect.

Some of this variation in the effects of blockers on C-type inactivation had nothing to do with blocking K^+ flow; variation occurred in the complete absence of K^+ ions. We measured the rate of inactivation with zero $[K^+]$ on both sides of the membrane and the effects of various blockers on this rate (Fig. 3C). The largest effect was produced by TEA, which slowed inactivation by about fivefold. Two other low-affinity blockers (C_3-TEA and QX-314) had similar but smaller effects. A small (about 1.5-fold) enhancement of the rate was induced by C_8-TEA and C_{10}-TEA, whereas C_4-TEA, C_6-TEA, and bretylium (Br) had no effect. These allosteric effects of the blockers in the absence of K^+ were small and in a few cases opposite to the overall effect of the blocker on inactivation when internal K^+ was present (compare Fig. 3B). Two blockers with no allosteric effect, C_4-TEA and C_6-TEA, caused substantial but different degrees of increase in the rate of inactivation. Thus, it appeared that the dominant effect of all blockers except TEA depended on the presence of internal K^+ and that the effect varied among the blockers.

We hypothesized that this variation might arise from the different dwell times of the blockers. Roughly speaking, long-lived blockers would prevent K^+ flow long enough to affect the occupancy of the control site, whereas short-lived blockers would not. To test this correlation, we first determined the kinetics of blockade from relaxation or noise analysis and then plotted the effect for each blocker against its dwell time (Fig. 3D). The inactivation rate for each blocker in the presence of K^+ was normalized to the rate for that blocker in the absence of K^+, thus isolating the component of the blocker effect that could be attributed to K^+ depletion.

The effects of the blockers were well correlated with their dwell times. Short-lived blockers produced less increase in the inactivation rate than long-lived blockers; as the dwell time increased, the inactivation rate became faster and asymptomatically approached a maximum rate. The half-maximal effect occurred at a blocker dwell time of ~150 μs (Fig. 3D).

Where does this characteristic dwell time come from? For a blocker with this dwell time, the control site would be occupied by a K^+ ion for about half of the total duration of the blocker's residence and would be empty for the other half; after that, the blocker would dissociate, and outward K^+ flux would flood the site with fresh K^+ ions. Accordingly, the occupancy of the control site would adjust to the blocked state of the channel with an average time of 150 μs. Although this seems fast, it takes much longer than the average time that a single K^+ ion resides in the pore during active permeation, about 0.1 μs. Even if we envision a cloud of accumulated K^+ ions in the outer entryway of the pore, this cloud should dissipate by diffusion in <1 μs (*11*). Thus, the rate-limiting step that determines the occupancy of the control site is likely to be the actual rate of release of K^+ from the control site.

Because this site is highly selective for K^+ over Na^+ ions (*12*), we propose that the site controlling the rate of C-type inactivation is one of the K^+ binding sites involved in permeation. On average, any permeation site must unbind ions at the throughput rate of the channel, about 10^7 s^{-1}. However, K^+ channels are known to have multiple K^+ ions moving in single file (*13*) with repulsive interactions between them. In theory [and by analogy with multi-ion permeation in Ca^{2+} channels (*14*)], a channel with only a single K^+ ion remaining would hold that ion much tighter than a channel with two K^+ ions. Thus, this last K^+ ion to leave the pore would have a dwell time of 150 μs (that is, an exit rate of 6700 s^{-1}), and the effect of blocker dwell time on the rate of C-type

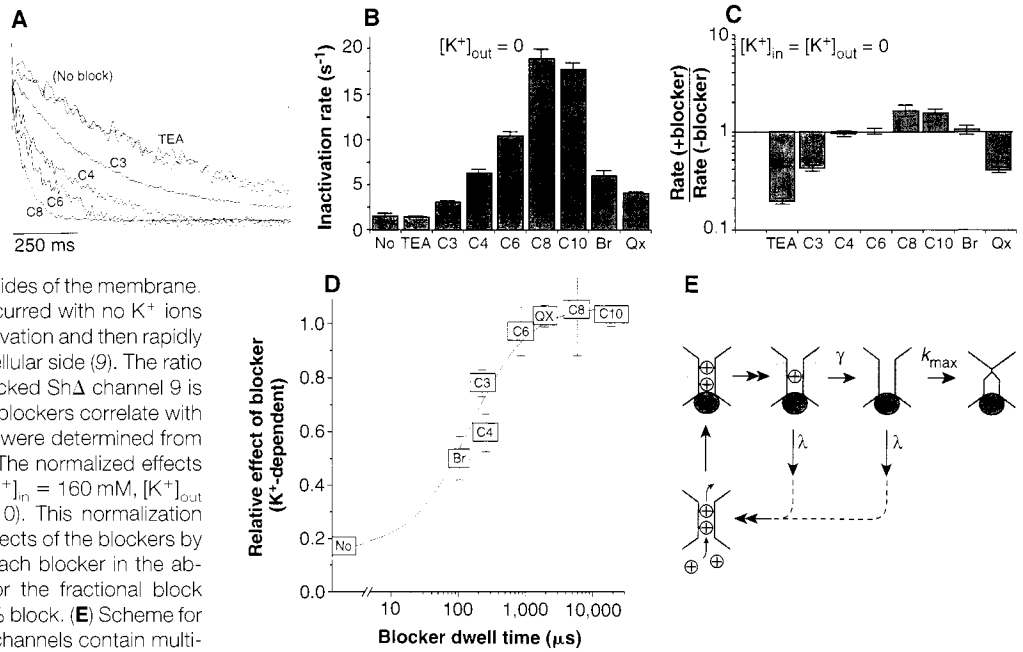

Fig. 3. Effects of blockers correlate with their dwell time in the channel. (**A**) C-type inactivation for ShΔ with various blockers, with zero external $[K^-]$ and normal internal $[K^-]$. The concentrations of all blockers were adjusted to give about 90% block. (**B**) Bar graph of rates from (A) and additional rates for C_{10}, bretylium (Br), and QX-314 (QX). No, no block. (**C**) Allosteric effects of blockers on C-type inactivation in the complete absence of K^- ions on both sides of the membrane. To assay the amount of inactivation that occurred with no K^+ ions present, we allowed various periods for inactivation and then rapidly perfused to restore normal $[K^-]$ to the intracellular side (*9*). The ratio of the rate with blocker to the rate for unblocked ShΔ channel 9 is plotted on a logarithmic scale. (**D**) Effects of blockers correlate with their dwell times in the channel. Dwell times were determined from noise analysis (*20*) or from relaxation rates. The normalized effects are given by the formula (rate with blocker, $[K^+]_{in}$ = 160 mM, $[K^+]_{out}$ = 0)/(rate with blocker, $[K^-]_{in}$ = $[K^-]_{out}$ = 0). This normalization isolates the variation in the K^+-dependent effects of the blockers by dividing by the maximal rate observed for each blocker in the absence of K^-. The rates were corrected for the fractional block (always about 90%) to give the effect at 100% block. (**E**) Scheme for blocker effects on inactivation. Conducting channels contain multiple K^+ ions and are rarely empty. When blockade begins, the first K^+ ion leaves quickly, at approximately the rate of throughput of permeation. The second K^+ ion, which no longer experiences repulsion, leaves more slowly, at rate γ. If blocker dissociation (with rate λ) is slow compared with γ, then the blocked channel spends most of its time empty of K^- ions and inactivation achieves its maximum rate k_{max}. The apparent rate of inactivation is given by $k_{app} = k_{max}\gamma/(\gamma + \lambda)$. This equation gives the solid line in (D), using a best fit value for the ion dissociation rate $\gamma = (150 \pm 30\ \mu s)^{-1}$. Dwell times (λ^{-1}) [shown in (D)] were the following: C_3-TEA, 234 ± 3 μs; C_4-TEA, 270 ± 10 μs; C_6-TEA, 880 ± 110 μs; C_8-TEA, 6 ± 1 ms; C_{10}-TEA, 19.1 ± 1.7 ms; Br, 110 ± 30 μs; QX, 2.0 ± 0.3 ms. No, no blocker added. All horizontal error bars are smaller than the symbols. TEA was not used because there was no net increase in the inactivation rate and the correction required would be prone to error.

inactivation would arise from a race between the dissociation of a blocker molecule and the dissociation of this K^+ ion (Fig. 3E) (*15*). In support of the idea that the control site is in the pore, we found a substantial voltage dependence for external K^+ binding to the blocked channel, with lower occupancy and thus faster inactivation at more positive voltages (electrical distance of 0.5 ± 0.1) (*16*).

Intracellular open channel blockers can produce use-dependent blockade of K^+ channels by promoting cumulative inactivation in two ways. First, blockade of outward K^+ flux leads to faster inactivation. This effect is sensitive to blocker dwell time and is opposed by external [K^+] in the physiologic range. Second, blockers can exert an allosteric effect on inactivation. Understanding the factors controlling the use dependence of K^+ channel blockers should help the development of better therapeutic agents, particularly in cases in which insufficient or even reverse use dependence is a serious problem for the therapeutic value and safety of channel blockers (*17*).

REFERENCES AND NOTES

1. R. L. Macdonald, *Epilepsia* **30**, S19 (1989); J. T. Bigger and B. F. Hoffman, in *The Pharmacological Basis of Therapeutics*, A. G. Gilman, L. S. Goodman, R. W. Rall, F. Murad, Eds. (Macmillan, New York, 1985), chap. 31.
2. The two accepted models for use-dependent blockade either use an increased affinity of the binding site in the open or inactivated state (the "modulated receptor" model) or trap the blocker in the channel by a closed gate (the "guarded receptor" model) [B. Hille, *J. Gen. Physiol.* **69**, 497 (1977); C. F. Starmer, A. O. Grant, H. C. Strauss, *Biophys. J.* **46**, 15 (1984); J. F. Butterworth and G. R. Strichartz, *Anesthesiology* **72**, 711 (1990)].
3. N-type inactivation occurs by a ball-and-chain mechanism in which the NH_2-terminal portion of the protein acts as a tethered blocker to inactivate the channel [T. Hoshi, W. N. Zagotta, R. W. Aldrich, *Science* **250**, 533 (1990); S. D. Demo and G. Yellen, *Neuron* **7**, 743 (1991)].
4. K. L. Choi, R. W. Aldrich, G. Yellen, *Proc. Natl. Acad. Sci. U.S.A.* **88**, 5092 (1991).
5. T. Hoshi, W. N. Zagotta, R. W. Aldrich, *Neuron* **7**, 547 (1991); G. Yellen, D. Sodickson, T.-Y. Chen, M. E. Jurman, *Biophys. J.* **66**, 1068 (1994).
6. C. M. Armstrong, *J. Gen. Physiol.* **54**, 553 (1969).
7. Abbreviations for the blockers are TEA, tetraethylammonium; C_n-TEA, alkyl (C_nH_{2n+1}) triethylammonium; Br, bretylium; and QX, QX-314 (a quaternary lidocaine derivative with a triethylamino moiety).
8. K. L. Choi, C. Mossman, J. Aubé, G. Yellen, *Neuron* **10**, 533 (1993).
9. T. Baukrowitz and G. Yellen, *ibid.* **15**, 951 (1995).
10. There is a noticeable dependence of inactivation rate on external K^+ under normal conditions of K^+ efflux, but this is much smaller than the effect noted here. It is more pronounced in mutants of the Shaker channel or in other K^+ channels [J. López-Barneo, T. Hoshi, S. H. Heinemann, R. W. Aldrich, *Recept. Channels* **1**, 61 (1993); L. A. Pardo *et al.*, *Proc. Natl. Acad. Sci. U.S.A.* **89**, 2466 (1992); P. Labarca and R. MacKinnon, *Biophys. J.* **61**, A378 (abstr.) (1992)]. Also, the effect of external K^+ in preventing blocker-promoted inactivation was not caused by knock-off of the blockers [as seen, for example, in C. M. Armstrong, *J. Gen. Physiol.* **58**, 413 (1971), and G. Yellen, *ibid.* **84**, 187 (1984)]. This could be ruled out because the degree of blockade did not change with the low concentrations of external K^+, and because there was no difference in the apparent affinity for K^+ measured in either the presence or the absence of blocker (so long as there was no outward flux).
11. B. Hille, *Ionic Channels of Excitable Membranes* (Sinauer, Sunderland, MA, ed. 2, 1992), chap. 11; J. Crank, *The Mathematics of Diffusion* (Clarendon Press, Oxford, UK, ed. 2, 1975).
12. Although most of the experiments presented here were done with external *N*-methylglucamine (NMG), the presence of external Na^+ made no detectable difference (*9*; T. Baukrowitz and G. Yellen, unpublished data).
13. A. L. Hodgkin and R. D. Keynes, *J. Physiol. (London)* **128**, 61 (1955); B. Hille and W. Schwarz, *J. Gen. Physiol.* **72**, 409 (1978).
14. W. Almers and E. W. McCleskey, *J. Physiol. (London)* **353**, 585 (1984); P. Hess and R. W. Tsien, *Nature* **309**, 453 (1984).
15. If more than two K^+ ions are involved in permeation, we cannot be certain that the dwell time we measure is that of the very last K^+ ion remaining: It could be that of the penultimate ion, for example, but not that of the first ion to leave (which must proceed at the rate of permeation).
16. T. Baukrowitz and G. Yellen, data not shown.
17. L. M. Hondeghem and D. J. Snyders, *Circulation* **81**, 686 (1990); but see T. J. Colatsky, C. H. Follmer, C. F. Starmer, *ibid.* **82**, 2235 (1990).
18. Transfection and electrophysiology methods were as previously described (*9*). The basic internal solution was 160 mM KCl, 1 mM EGTA, 0.5 mM $MgCl_2$, and 10 mM Hepes (pH 7.4); in the zero internal [K^+] experiments, K^+ was replaced with NMG. The external solution for Fig. 1, A and D, contained 150 mM NaCl, 3 mM $CaCl_2$, 1 mM $MgCl_2$, and 10 mM Hepes (pH 7.4), and KCl was added at the indicated concentration. All of the other experiments used 160 mM NMG, 3 mM $CaCl_2$, 1 mM $MgCl_2$, and 10 mM Hepes (pH 7.4), in which KCl was substituted for NMG as indicated.
19. Copper (II):phenanthroline (750 μM:3 mM) was applied to the intracellular face of the patch for <1 min to eliminate N-type inactivation [J. P. Ruppersberg *et al.*, *Nature* **352**, 711 (1991)].
20. Power spectra from long pulses were computed by fast Fourier transform (Matlab; Mathsoft, Natick, MA) and fitted to a sum of Lorentzian and $1/f$ noise, where f is the frequency. The corner frequency and fractional block were used to compute the off-rate of the blocker.

21. We thank M. Jurman for providing transfected cells and C. Miller for his trenchant advice on the manuscript. Supported by National Institute of Neurological Diseases and Stroke grant NS29693 (G.Y.) and by a stipend from the Gottlieb Daimler-Karl Benz Foundation (T.B.).

15 August 1995; accepted 8 November 1995

Horizontal Cells of the Primate Retina: Cone Specificity Without Spectral Opponency

Dennis M. Dacey,* Barry B. Lee, Donna K. Stafford, Joel Pokorny, Vivianne C. Smith

The chromatic dimensions of human color vision have a neural basis in the retina. Ganglion cells, the output neurons of the retina, exhibit spectral opponency; they are excited by some wavelengths and inhibited by others. The hypothesis that the opponent circuitry emerges from selective connections between horizontal cell interneurons and cone photoreceptors sensitive to long, middle, and short wavelengths (L-, M-, and S-cones) was tested by physiologically and anatomically characterizing cone connections of horizontal cell mosaics in macaque monkeys. H1 horizontal cells received input only from L- and M-cones, whereas H2 horizontal cells received a strong input from S-cones and a weaker input from L- and M-cones. All cone inputs were the same sign, and both horizontal cell types lacked opponency. Despite cone type selectivity, the horizontal cell cannot be the locus of an opponent transformation in primates, including humans.

The retina is the site of two fundamental stages in the neural representation of color. First, the visual image is discretely sampled by three types of cone photoreceptor with different spectral sensitivities (*1*). Only 7 to 10% of the cones are S-cones (*2*); the remainder are L- and M-cones. Second, cone signals interact antagonistically to form spectrally opponent pathways (*3*). In a red-green pathway, signals from L- and M-cones are differenced, and in a blue-yellow pathway, signals from S-cones oppose a combined signal from L- and M-cones. For nearly 40 years, it has been known that these opponent signals are a property of retinal ganglion cells, the output neurons of the retina, yet the interneuronal circuitry that creates the opponent transformation has remained virtually unstudied because of the technical difficulties of making intracellular recordings from the intact retina of primates (*4*, *5*).

In nonmammals with trichromatic vision, horizontal cells—one class of interneuron—display spectral opponency (*6*). A long-held view is that an opponent transformation occurs by cone type–selective negative feedback from horizontal cells to cones (*7*). Indirect evidence for such opponent feedback in primates is conflicting. Boycott and Wässle reported that two horizontal cell types (H1 and H2) contact all cone types nonselectively and should not, therefore, subserve opponency (*8*); the first

D. M. Dacey and D. K. Stafford, Department of Biological Structure, Box 357420, University of Washington, Seattle, WA 98195–7420, USA.
B. B. Lee, Max Planck Institute for Biophysical Chemistry, 37077 Göttingen, Germany.
J. Pokorny and V. C. Smith, Visual Sciences Center, University of Chicago, Chicago, IL 60637, USA.
*To whom correspondence should be addressed.